

Tutorial on shell model calculations and the production of nuclear Hamiltonians

A. Signoracci*

Centre de Saclay, IRFU/Service de Physique Nucléaire, F-91191 Gif-sur-Yvette, France

T. Duguet†

*National Superconducting Cyclotron Laboratory and Department of Physics and Astronomy,
Michigan State University, East Lansing, MI 48824, USA*

J. D. Holt‡

*Institut für Kernphysik, Technische Universität Darmstadt, 64289 Darmstadt, Germany and
ExtreMe Matter Institute EMMI, GSI Helmholtzzentrum für Schwerionenforschung GmbH, 64291 Darmstadt, Germany*

* angelo.signoracci@cea.fr

† thomas.duguet@cea.fr

‡ holt@theorie.ikp.physik.tu-darmstadt.de

Tutorial of the *Espace de Structure Nucléaire Théorique*

13 May - 17 May 2013

CEA/SPhN, Orme des Merisiers, build. 703, room 135, F-91191 Gif-sur-Yvette Cedex

I. PROBLEM SET SOLUTIONS

Many figures are included at the end of the file for a clearer presentation of results. Some of these files are created automatically by NUSHELLX, such that a good test of your calculations is to reproduce, for example, Figures 2 and 3.

IMPORTANT!!! Results below are not necessarily exact. Various “hidden” parameters such as the convergence criteria and the number of states calculated by default change in different versions of NUSHELLX and can slightly affect the results (in energies, on the keV level; in other properties, usually at the level of a few %). All results given below were obtained in April 2012. With the most recent version of the code (obtained from Alex Brown in May 2013), the results are slightly different. For example, the $B(GT)$ values of Problem Set 3, Question 1 are 0.359, 0.200, and 1.083 for the three lowest $1+$ states. If your calculations are nearly but not identically equal, you have likely performed the calculations correctly.

Problem Set 1

1. $A = 24$ nuclei
 - (a) No answer required
 - (b) See Figure 1. All assigned experimental states have a corresponding theoretical state within about twice the rms deviation of 126 keV for the USDB interaction. The predicted J^π value for the state at 4.886 MeV in ^{24}Ne is 3^+ (there are two theoretical states nearby in energy, and the 0^+ has a corresponding experimental state. This leaves the 3^+ state at 4.81 MeV to connect to the experimental state). The two states at 5.636 MeV and 5.653 MeV should correspond to the theoretical 3^+ and 4^+ states at 5.43 MeV and 5.69 MeV, respectively. Hoffman et al. [Phys. Rev. C **68**, 034304 (2003)] have since assigned J^π values for these three experimental states, agreeing with the three assignments from comparison to the USDB interaction. The experimental 4^+ state is the 5.653 MeV state.
 - (c) The symmetry of the USDB interaction can be seen by comparing the $T_z = \pm 2$ level schemes of ^{24}Ne and ^{24}Si , especially in the .lpt files. The level schemes are identical in these nuclei. As the $T = 0$ nucleus, ^{24}Mg also has $T = 0, 1$ states that are not present in the other two nuclei and which enter at lower energy. The first $T = 2$ state in ^{24}Mg occurs at the same absolute energy as the ground states of ^{24}Ne and ^{24}Si (-71.725 MeV), but the ground state now has $T = 0$ with absolute energy -87.105 MeV. This places the first $T = 2$ state, which is the $12^{\text{th}}0^+$ state in ^{24}Mg , at an excitation energy of 15.38 MeV.
2. Mass of a nucleus
 - (a) The additional value required for this problem is the mass of ^{16}O , since all energies in the sd shell are calculated relative to the core. The ground state energy of ^{30}Al with the USDB interaction, including the Coulomb correction of 21.48 MeV, is -120.018 MeV. The experimental mass excess of -15872(14) keV can be converted to a binding energy by the included formulas, with the result of 247.84(1) MeV. Subtracting the 127.619 MeV binding energy of ^{16}O , the value of 120.22(1) MeV can be compared directly to the output in the al30b.lpt file. The USDB interaction is approximately 200 keV underbound. While this results in reasonable agreement relative to the uncertainty in the interaction, the result can be improved by treating the Coulomb interaction accurately in the reduced model space. This can be done by typing `sdpn` and `usdbcdpn` in shell for the model space and interaction. The binding energy of ^{30}Al is 120.314 MeV with this “USDB plus charge dependence” interaction. Notice that even though the Coulomb interaction is repulsive, we have gained 300 keV in binding energy by treating it accurately, with a final result within 95 keV of experiment.
3. Spectroscopic factors
 - (a) In the independent particle model, with the NUSHELLX sum rule corresponding to a total strength of $2j + 1$ for each orbit, we only need to determine how many protons and neutrons are occupied in ^{34}S . There are 16 protons and 18 neutrons, corresponding to 8 valence protons and 10 valence neutrons outside

the ^{16}O core. The $0d_{5/2}$ and $1s_{1/2}$ orbits are completely filled, while the $0d_{3/2}$ orbit is empty for protons and half-filled for neutrons. Therefore, the nonzero C^2S^\pm for ^{34}S are $C^2S^-(\pi d_{5/2}) = 6$, $C^2S^-(\nu d_{5/2}) = 6$, $C^2S^-(\pi s_{1/2}) = 2$, $C^2S^-(\pi s_{1/2}) = 2$, $C^2S^+(\pi d_{3/2}) = 1$, $C^2S^-(\nu d_{3/2}) = 2$, $C^2S^+(\nu d_{3/2}) = 0.5$.

- (b) The expected single particle configuration from the independent particle model has partition 6 for neutrons (A) and partition 12 for protons (B), which accounts for 52.33% of the calculated wavefunction. The next most likely configuration of protons is partition 3 with almost 10% of the wavefunction resulting from an excitation of the pair of $1s_{1/2}$ protons into the $0d_{3/2}$ orbit. 78.73% of the wavefunction comes from $J_p = J_n = 0$.
- (c) No answer required
- (d) The calculation is in better agreement with the more recent experiment from Khan et al. Note that spectroscopic factors are not experimental observables and depend on the reaction model used to extract them. It is better to compare theoretical calculations to experimental observables (e.g. cross sections), but reaction calculations are not straightforward within the shell model.

Results with the USDB interaction

E_x (MeV)	J	C^2S
0	$\frac{1}{2}$	1.30
1.455	$\frac{3}{2}$	0.51
1.959	$\frac{5}{2}$	0.99
3.438	$\frac{3}{2}$	0.02
3.648	$\frac{5}{2}$	0.27
4.078	$\frac{5}{2}$	1.39
5.124	$\frac{5}{2}$	1.69

4. Electromagnetic transitions

- (a) No answer required
- (b) No answer required
- (c) The results for the energies are in good agreement, at least up to ^{26}Ne . There are much larger variations for $B(E2)$ values, but some of the states are reproduced well. There does not seem to be much correlation between $E(2^+)$ and $B(E2)$, contrary to what has been suggested by empirical formulas, e.g. see Phys. Rev. C **66**, 067303 (2002). The largest disagreement between theory and experiment occurs for ^{30}Ne , and to a lesser extent ^{28}Ne , which are in and approaching the island of inversion region, respectively. The pf model space orbits are essential to reproduce the low-lying states in these nuclei. Note also that effective charges are employed in the calculation, but that the electric transition of ^{18}Ne consisting only of two valence protons is still not reproduced.

Results with the USDB interaction

^ANe	$E(2^+)$ (MeV)	$B(E2)(e^2\text{fm}^4)$
18	1.998	36.3
20	1.747	60.1
22	1.363	59.9
24	2.111	49.6
26	2.063	49.9
28	1.623	44.0
30	1.708	33.2

Problem Set 2

1. Selection of model space and interaction (part 1)

- (a) By the NUSHELLX naming scheme as found in label.dat, the model space should be fp.sp, since the doubly magic ^{40}Ca can be treated as a good vacuum reference state. There are multiple options for the interaction in this model space, but gx1 is one good choice reproducing data throughout the pf shell.
- (b) The states expected to be observed in an experiment measuring $^{48}\text{Ti}(d,t)^{47}\text{Ti}$ depend on the experimental details, but in general there are necessary truncations on excitation energy and spectroscopic factors. A reasonable answer to this question might pick cuts for $SF_{min} = 0.02$ and $E_{max} = 6$ MeV. This choice would result in nine measured states, including the lowest state of each possible spin (based on the chosen model space).
- (c) See Figure 2. Even though the calculated ground state spin of ^{47}Ti does not agree with the experimental value, the lowest calculated $\frac{5}{2}^-$ state is at 61 keV in excitation energy. Including the rms deviation of the gx1 interaction, the $\frac{5}{2}^-$ and $\frac{7}{2}^-$ could equally be expected to represent the physical ground state. The calculations suggest that the experimental state at 2.16 MeV, with unassigned spin, may actually be composed of multiple states with smaller spectroscopic factors. Experimentally, the state is identified by a peak in the observed events at a given energy, which then leads to an “experimental” SF of 0.12 based on a single-state reaction model. Theoretically, there are five states within the rms deviation whose SF add linearly to 0.09. To assess the spin and spectroscopic factors around 2.16 MeV, greater experimental resolution is required.

Results with the gx1 interaction

E_x (MeV)	J	C^2S
0.00	$\frac{7}{2}$	4.31
0.06	$\frac{5}{2}$	0.02
1.25	$\frac{3}{2}$	0.15
2.04	$\frac{1}{2}$	0.02
2.11	$\frac{5}{2}$	0.03
2.14	$\frac{3}{2}$	0.00
2.27	$\frac{3}{2}$	0.03
2.29	$\frac{7}{2}$	0.01
2.82	$\frac{7}{2}$	0.61
3.10	$\frac{7}{2}$	0.06

2. Selection of model space and interaction (part 2)

- (a) In the standard harmonic oscillator plus spin-orbit mean field, ^{11}Be would have a ground state spin of $\frac{1}{2}^-$ and a low-lying $\frac{3}{2}^-$ state. Calculations in the $N = 1$ oscillator shell (p -shell) would be expected to reproduce the behavior of this nucleus, since it lies between ^4He and ^{16}O .
- (b) To calculate positive and negative parity states, both the $N = 1$ and $N = 2$ shells are needed. This corresponds to the psd.sp model space in NUSHELLX. It is also possible to include all orbits up through the $N = 3$ oscillator shell using the spsdpf.sp model space.
- (c) With both the psdmk and psdmwk interaction in the psd model space, the ground state spin of ^{11}Be is $\frac{1}{2}^+$. The calculated energy difference between the $J^\pi = \frac{1}{2}^\pm$ states is 4.34 MeV with the psdmwk interaction and 4.88 MeV with the psdmk interaction. The agreement with experimental data is very poor for both interactions. We could argue that psdmwk is better since the $\frac{3}{2}^-$ state is at least reasonably reproduced in this case, but since both are 4 MeV off on the $\frac{1}{2}^-$ state, we should not place too much trust in either interaction. See Figure 3 for the results with the psdmwk interaction.

3. **Conceptual :** The results thus far were selected to show that results calculated in the shell model are not necessarily reliable, especially for very exotic nuclei. We can observe from the neon results and beryllium results that, as a function of the asymmetry, we should be wary of calculations where $N/Z \approx 2$. While showing instances where the shell model fails was important for our purposes, we should emphasize that the shell model does quite well throughout standard model spaces for a variety of properties.

Problem Set 3

1. Gamow-Teller transitions

- (a) The transitions from the 0^+ ground state in ^{28}Si can populate 0^+ and 1^+ states in ^{28}P . The energies are very well produced- only the theoretical 1_5^+ state does not correspond within the approximate uncertainty to a measured experimental state. In the *.bgt file, we can see that this state has a very small B(GT) value (although it is larger than that of the eighth and tenth 1^+ states). The B(GT) values are typically much larger than the experimental values, especially for the low-lying states where we observe double the strength theoretically.

Results with the USDB interaction

E_x (MeV)	$B(GT)$
1.20	0.356
1.50	0.200
2.07	1.077
3.00	0.466
3.59	0.052
3.90	0.208
4.85	0.878
5.17	0.015
5.80	0.386
6.01	0.000

- (b) From Lecture IV, beta decay values can be determined from the equation

$$ft_{1/2}^{k,k'} = \frac{C}{B_{k,k'}(F_{\pm}) + (g_A/g_V)^2 B_{k,k'}(GT_{\pm})},$$

where Fermi decay does not contribute for 1^+ states in ^{28}P . There is a program in NUSHELLX that can be run to produce $\log ft$ values, which we did not cover in the lectures. It can be run by typing `betadecay x <enter>` in Windows with an input file `x.beq` (an example can be found in the beta folder in the app directory). For most calculations of interest, there is already a way to calculate it in NUSHELLX, even if there is no documentation. Feel free to ask for help based on your calculation of interest.

2. Approximations

- (a) See Figure 4 for reference during parts (a)-(c) of this question. In the sd model space, we would expect to reproduce the low-lying positive parity states, so at least the ground state and first excited state at 50 keV. Depending on the trust placed in assigning levels, you might also consider the experimental states at 0.67, 0.94, 2.24, 3.76, and 3.81 MeV as positive parity.
- (b) The ground state is $\frac{3}{2}^+$, but the first $\frac{1}{2}^+$ state is above 2 MeV with the USDB interaction, so the nearly degenerate experimental levels are not reproduced. The rest of the level scheme is poorly reproduced as well. For example, there are eight experimental excited states before the first excited level with USDB, although only the positive parity states can be reproduced in the sd model space.
- (c) The agreement with respect to experiment has improved with this new interaction which I will call `usdbed`, as the $\frac{1}{2}^+$ and $\frac{3}{2}^+$ doublet is now reproduced. The experimental level density below 1.5 MeV is still much greater than the theoretical one. The modification of the interaction, in this case the one-body component, means that the interaction is no longer designed to reproduce the entire sd shell. While we may have improved the results for one nucleus of interest, there are many parameters that can be adjusted to reproduce the low-lying states in one nucleus. If we now look at calculations throughout the sd shell, this new interaction is not necessarily appropriate as we no longer understand how the values are being

constrained. For example, a calculation of ^{33}P with the usdbed interaction as shown in Figure 5 does not reproduce the ground state or level scheme, while the standard USDB interaction does quite well.

- (d) The binding energy of the experimental state at 50 keV excitation energy is 243.99 MeV, in comparison to the USDB calculation of 243.36 MeV including the ^{16}O vacuum energy and the Coulomb correction. The experimental $3/2^+$ state at 50 keV does not seem to correspond to the calculated ground state with the USDB interaction, but the experimental state at 673 keV has a binding energy of 243.32 MeV, in good agreement. This motivated the assignment of $J^\pi = \frac{3}{2}^+$ for the 673 keV state by Miller et al.
- (e) Even including a larger model space that enables the calculation of negative parity states in the calculation, the experimental data is not reproduced well. The $\frac{1}{2}^+$ state is still too high in energy, and the high level density at low excitation energy is not reproduced. We should recall the problems away from stability, especially in the island of inversion region, observed already.

3. Decays and the dripline

- (a) The agreement with experimental data is excellent for the USDB interaction, even beyond the neutron dripline ($N = 16$) and for unbound states. See Figure 6 for compiled results.
- (b) For $^{20,21,22}\text{O}$, the ground state decays by beta decay and the excited states gamma decay to the ground state. For ^{23}O , the ground state decays by beta decay but the excited $\frac{5}{2}^+$ and $\frac{3}{2}^+$ states are higher in energy than the ^{22}O ground state, and therefore decay by neutron emission. Similarly, the ground state of ^{24}O beta decays while the excited 2^+ state neutron decays. The ground state of ^{25}O is unbound and decays by neutron emission. The ground state of ^{26}O is bound to one-neutron emission, but unbound to two-neutron emission and decays to the ground state of ^{24}O . The ground states of $^{27,28}\text{O}$ are both unbound to emissions involving neutrons, and decay to ^{24}O either directly or through ^{26}O .
- (c) If three-body forces are needed to reproduce the behavior of oxygen isotopes near the dripline, then the USDB interaction must account for three-body forces in some way. While it only consists of one-body (SPE) and two-body (TBME) components, the three-body force can be decomposed into an effective one-body, effective two-body, and explicit three-body term. The explicit three-body term is small relative to the others, and so the empirical fitting procedure to energy data in the sd shell reproduces the effective behavior of three-body forces. For comparison, a microscopic procedure starting from the NN interaction can produce an effective sd shell interaction (as in Problem Set 4 and Lectures V-VII) which has no three-body component, and the difference can be related to three-body forces (relative to the uncertainty in the renormalization group methods and many-body perturbation theory).

Problem Set 4

1. Application to standard model space

- (a) No answer required. For reference, I will denote the derived effective interaction with ^{16}O as the target by o16 and that with ^{28}Si as the target by si28.
- (b) The two interactions are relatively similar to each other, typically, the TBME of si28 are weaker by about 10%. The difference between the two interactions is due to whether the $0d_{5/2}$ orbit is occupied or not, which affects the evaluation of, for example, the core-polarization diagram at second order in perturbation theory. A much smaller effect is due to the mass dependence of the harmonic oscillator basis which is employed in the procedure.
- (c) The appropriate matrix elements for comparison are the neutron-neutron TBME, since the USDB interaction does not include the Coulomb interaction, which is significant for protons. Comparing the USDB values to those of the two derived interactions, we see that many TBME are in good agreement, e.g. $\langle 0d_{5/2}0d_{5/2} | V_{ms} | 0d_{5/2}0d_{5/2} \rangle_{J=0} = -2.64(-2.52)[-2.55]$ for o16 (si28) [USDB]. However, there are many TBME where the USDB values are drastically different, e.g. $\langle 0d_{3/2}0d_{3/2} | V_{ms} | 0d_{3/2}0d_{3/2} \rangle_{J=0} = -0.76(-1.11)[-1.90]$ for o16 (si28) [USDB] and all the $J = 3$ TBME.
- (d) The level density is higher with the o16 and si28 interactions, even though the yrast states are still reproduced relatively well. The results for the o16 interaction are shown in Fig. 7 for comparison to Fig. 1.
- (e) The empirical interaction performs much better than the produced effective interactions. Since the empirical interaction is parameterized and fit to energy data throughout the sd shell, interactions determined in a

microscopic way will always fare worse in comparison to experiment, at least within the range of data included in the fitting procedure. While a microscopic procedure is desired and leads to a better understanding of the contributions to the effective interaction (e.g., how much core polarization contributes to specific TBME), there are practical limitations to this procedure. Most importantly, three-body forces (and higher) are excluded from the start, as a microscopic nucleon-nucleon potential is used as input. Furthermore, restrictions on the order of perturbation theory and number of excitations, given in $\hbar\omega$, limit the accuracy of the effective interaction in the reduced model space. However, one benefit of the microscopic effective interactions is that isospin symmetry is broken from the Coulomb, CIB, and CSB interactions from the nucleon-nucleon interaction, so the level schemes of ^{24}Si and ^{24}Ne are not identical, like experiment.

2. Application to exotic isotopes

- (a) An appropriate model space requires the sd proton orbits and at least some, if not all, of the sd and pf neutron orbits. The closest neutron orbits to the Fermi energy are $0d_{3/2}, 0f_{7/2}, 1s_{1/2}, 1p_{3/2}$.
- (b) No answer required
- (c) The results for ^{30}Ne with this new interaction (I will refer to it as si34hf) have improved significantly relative to USDB. The $B(E2)$ transition is $65.0 e^2\text{fm}^4$, in comparison to the experimental value of $92.0 e^2\text{fm}^4$. The energy is still about 1 MeV too high, like the USDB calculation, but the included pf orbits seem to include necessary wavefunction information. For ^{31}Mg , the si34hf interaction now produces positive and negative parity states, but the low-energy level density is still too small and the $\frac{1}{2}^+$ state is still much too high in energy, but the improvement over both empirical interactions is clear.
- (d) **Optional question for future investigation :** Going to 6 $\hbar\omega$ excitations reduces the 2^+ energy in ^{30}Ne by 100 keV and increases the $B(E2)$ value to $70.3 e^2\text{fm}^4$. Increasing the number of excitations produces a stronger interaction, like increasing the order of perturbation theory (see Lecture VII). Employing 8-10 $\hbar\omega$ excitations and third order of perturbation theory represents the cutting edge of nuclear structure calculations, but also requires significant computing power to achieve the result. Even in this case, the agreement with experiment may not be satisfactory (I haven't computed the result), but it is a significant improvement on the USDB result. The inclusion of three-body forces and the improvement of the one-body SPE component are necessary to reproduce experimental data consistently.

The effect on the calculations with a different model space depends on the specific choice of model space. If the agreement with experiment is worse, perhaps the model space is too restrictive or the effective interaction was not determined properly (recall discussion from Lecture VII about divergences in large model spaces). In terms of the calculation, there is always a tradeoff between inclusion of degrees of freedom and the amount of CPU time required. In general, a larger model space will require more time to calculate these nuclei but will also include more degrees of freedom which may be of interest to the problem; for instance, in this problem, the $0d_{5/2}$ and $1p_{1/2}$ neutron orbits might contribute significantly to the calculated results.

Problem Set 5

1. Here we will compare the monopoles of a phenomenological model and those of a microscopic interaction to gauge the character of physics missing from our theory.
 - (a) From the USDB phenomenological interaction, the $T = 1$ monopoles in MeV are
 - $d_{5/2}d_{5/2}$ -0.628
 - $d_{5/2}d_{3/2}$ -0.268
 - $d_{5/2}s_{1/2}$ 0.007
 - $d_{3/2}d_{3/2}$ -0.398
 - $d_{3/2}s_{1/2}$ 0.004
 - $s_{1/2}s_{1/2}$ -1.691
 - (b) Checking against the next part will ensure this was done correctly
 - (c) Results may vary slightly depending on the interaction chosen, but the values for a low-momentum interaction beginning from the standard chiral N^3LO interaction to 2nd order in MBPT are :
 - $d_{5/2}d_{5/2}$ -0.585
 - $d_{5/2}d_{3/2}$ -0.661
 - $d_{5/2}s_{1/2}$ -0.416

$$d_{3/2}d_{3/2} -0.136$$

$$d_{3/2}s_{1/2} -0.039$$

$$s_{1/2}s_{1/2} -2.430$$

We see that generally for monopoles involving lower-lying orbitals (i.e., $d_{5/2}$ and $s_{1/2}$), the microscopic monopoles are more *attractive* than those given from phenomenology. Therefore we expect that additional *repulsion* will be needed in order to improve the predictions of the microscopic theory.

2. No answer required, just following the instructions. This will allow us to calculate a simple density-dependent three-nucleon interaction. If done correctly it's our hope that this correction will provide in part some of the missing physics needed to improve our theory (i.e. agreement with data).
3. Again, no answer required. Checking against the figure will ensure the steps were followed correctly. First of all we should notice that all partial waves vanish beyond S -waves (i.e., only 1S_0 and 3S_1 channels have nonzero matrix elements). This would be expected since the contact interaction is spherically symmetric and all other partial waves are not. Comparing with Figure 8 we should confirm that these results agree with line 6, which denotes the contact 3N interaction.
4. The monopoles from this 3N contact interaction are

$$d_{5/2}d_{5/2} 0.547$$

$$d_{5/2}d_{3/2} 0.106$$

$$d_{5/2}s_{1/2} 0.197$$

$$d_{3/2}d_{3/2} 0.841$$

$$d_{3/2}s_{1/2} 0.197$$

$$s_{1/2}s_{1/2} 1.395$$

As expected, these are uniformly positive, so, if not too large, should bring our microscopic monopoles much closer to the phenomenological values. However, if we compare with the difference between the USDB monopoles and those of the low-momentum interaction :

$$d_{5/2}d_{5/2} -0.043$$

$$d_{5/2}d_{3/2} 0.375$$

$$d_{5/2}s_{1/2} 0.423$$

$$d_{3/2}d_{3/2} -0.262$$

$$d_{3/2}s_{1/2} 0.043$$

$$s_{1/2}s_{1/2} 0.739$$

Ignoring the high-lying monopoles, we see that the current 3N contact interaction gives too much repulsion by more than a factor of two. The parameters of the EN contact interaction can be modified to optimize the agreement with experiment (i.e. to reproduce the USDB values approximately).

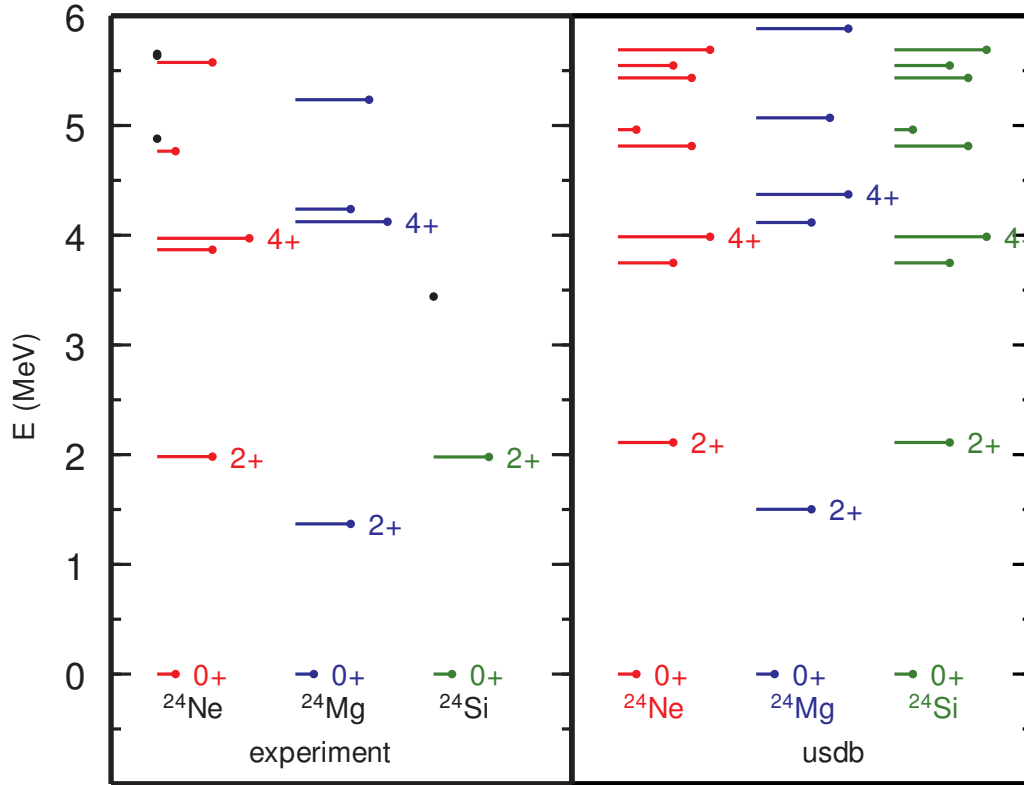


FIGURE 1. Comparison of the level schemes for experiment (left) and for the USDB interaction (right) for the $A = 24$ nuclei of interest in this problem. For this and similar plots below, the length of the line corresponds to the angular momentum of the state, with a label each time a highest J value occurs, starting from the ground state. Therefore, the ground state spin is always labeled. Experimental states are taken from the ENSDF database unless otherwise cited. States in the ENSDF database without an assigned J^π value are plotted as black dots at the appropriate energies. The level schemes are displayed up to 6 MeV, although the theoretical level scheme includes a finite number of states for a given J^π value (ten unless otherwise noted). As a result, nuclei with a high density of states might not show the full theoretical level scheme through 6 MeV.

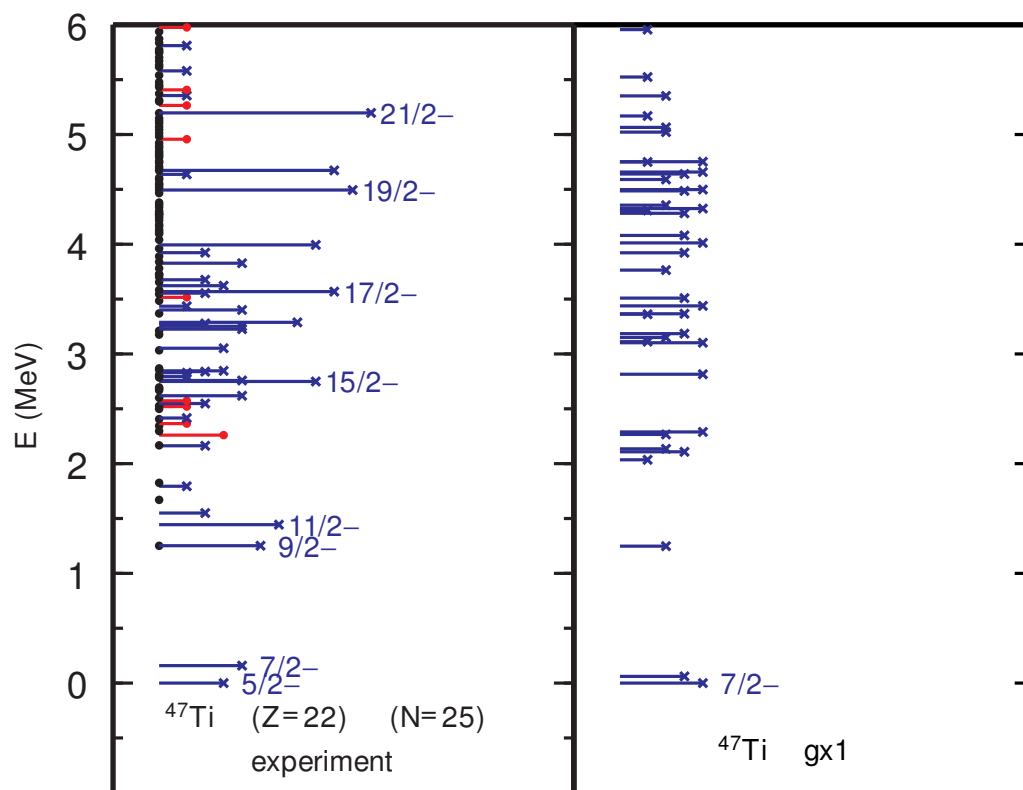


FIGURE 2. The level schemes for ^{47}Ti for experiment (left) and with the gx1 interaction in the pf model space (right). Note that only states up to $J = \frac{7}{2}$ are calculated, as demanded in the problem set. See also the caption to Fig. 1.

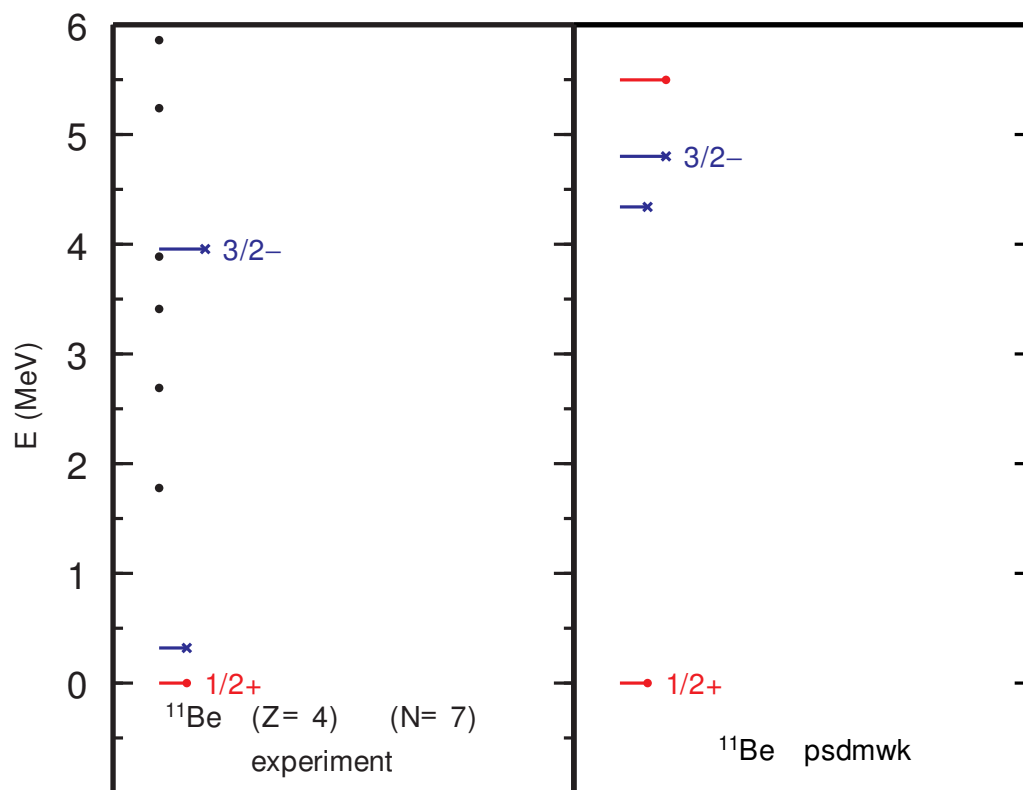


FIGURE 3. The level schemes for ^{11}Be for experiment (left) and with the *psdmwk* interaction in the *psd* model space (right). Note that only states up to $J = \frac{3}{2}$ are calculated, as demanded in the problem set. See also the caption to Fig. 1.

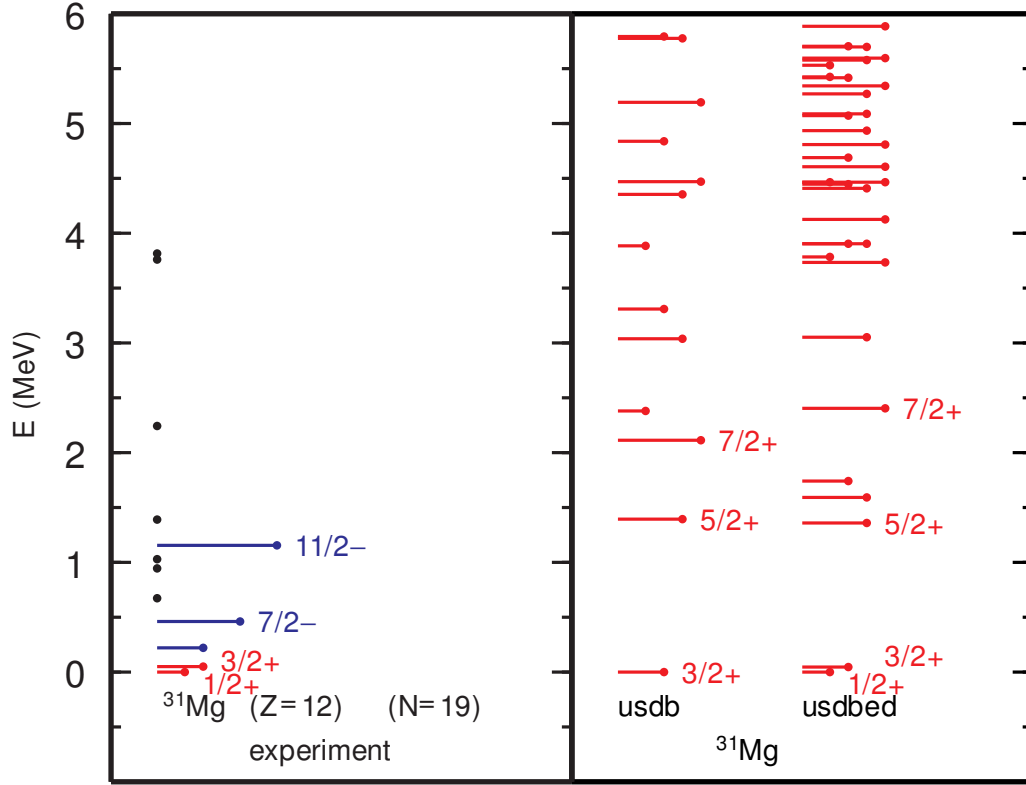


FIGURE 4. Level schemes for ^{31}Mg for experiment (left) and theory (right). On the left, I have assigned J^π values using weak selection rules from ENSDF. On the right, results are shown with both the USDB interaction and a modified interaction with different SPE components (usdbed). See also the caption to Fig. 1.

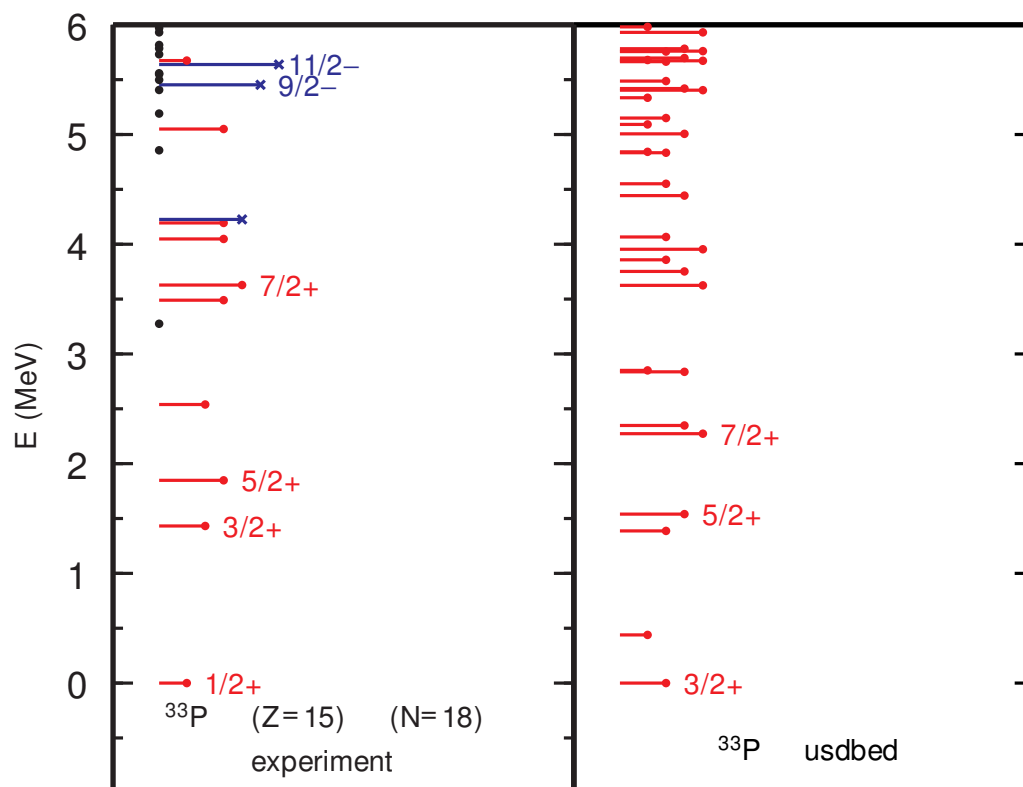


FIGURE 5. Level schemes for ^{33}P for experiment (left) and with the usdbed interaction (right). Even though the results for ^{31}Mg were significantly improved with this new interaction, the change in SPE affects the results throughout the sd shell. See also caption to Fig. 1.

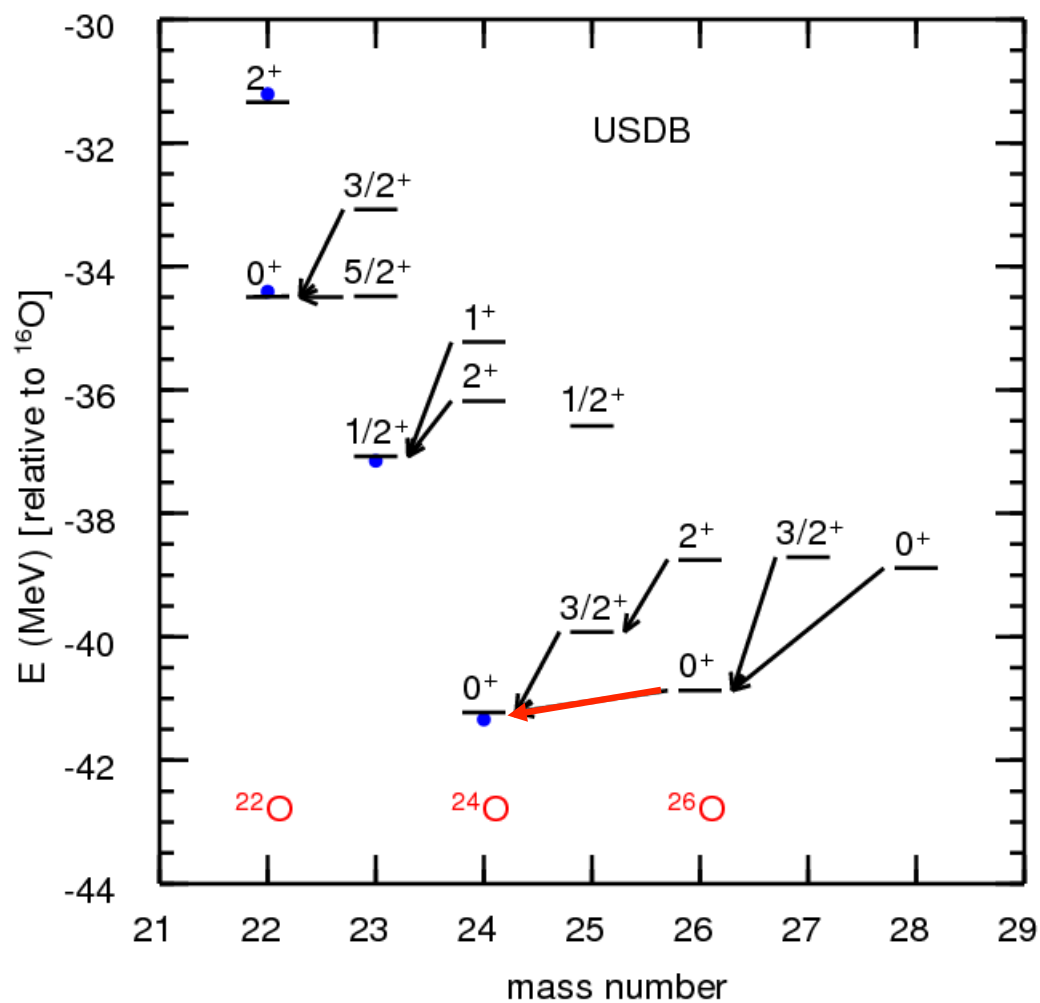


FIGURE 6. Comparison of USDB results to available experimental data in the neutron-rich oxygen isotopes. Figure courtesy of Alex Brown.

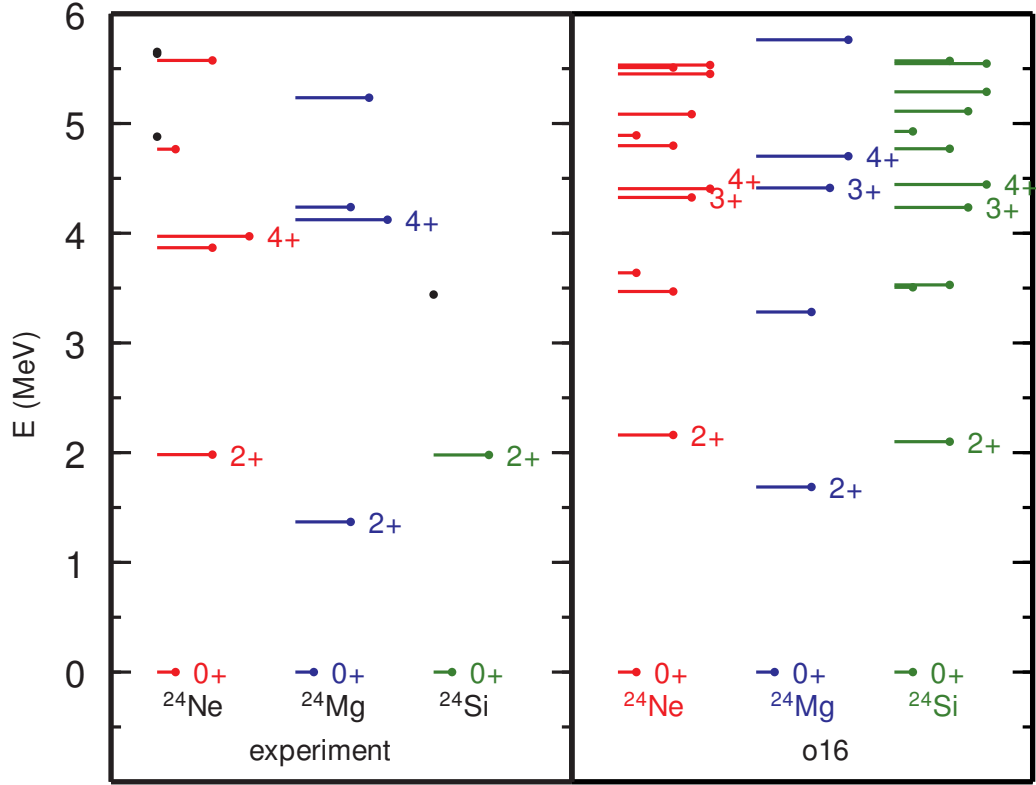


FIGURE 7. Comparison of the level schemes for experiment (left) and for the o16 interaction (right) for the $A = 24$ nuclei of interest in this problem. See also caption to Fig. 1.

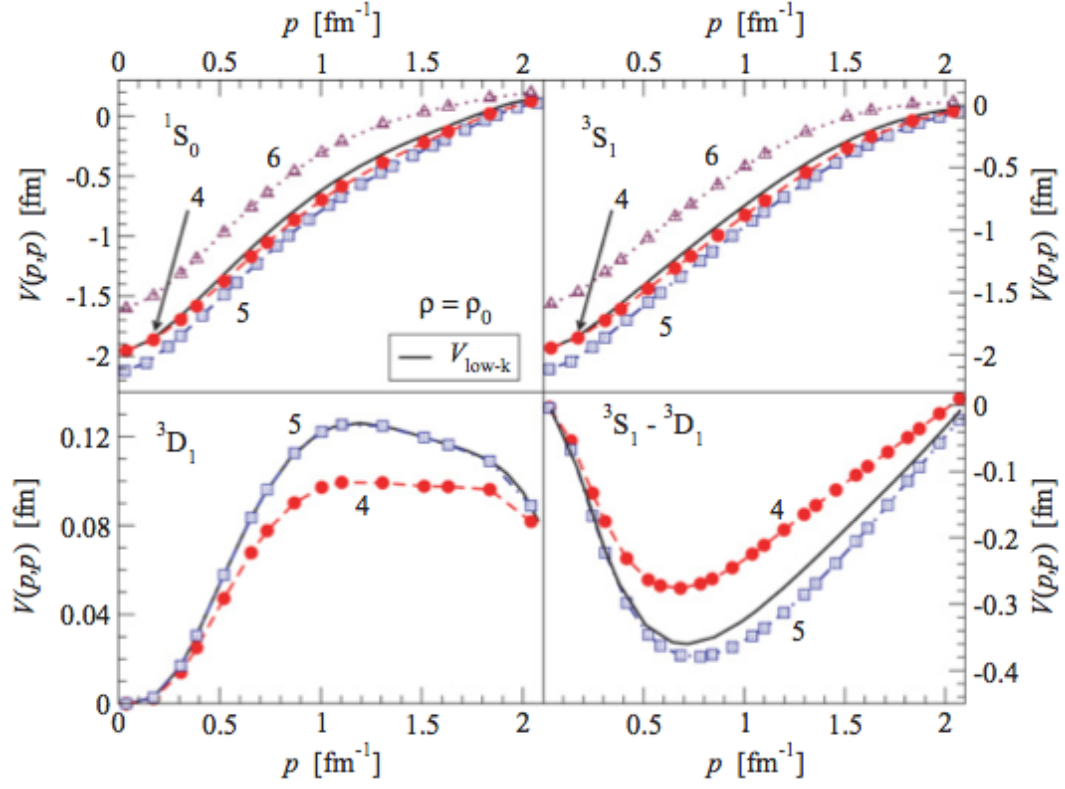


FIGURE 8. Plot of partial wave matrix elements of various density-dependent 3N contributions.